LAWRENCE
LIVERMORE
NATIONAL
LABORATORY

UCRL-CONF-205522

Synchrotron x-ray study of multilayers in Laue geometry

H. C. Kang, G. B. Stephenson, C. Liu, R. Conley, A. T. Macrander, J. Maser, S. Bajt, H. N. Chapman

July 27, 2004

SPIE's 49th Annual Meeting
Denver, CO, United States
August 2, 2004 through August 6, 2004

UCRL-CONF-205522

Synchrotron x-ray study of multilayers in Laue geometry

H. C. Kang[a], G. B. Stephenson[a*], C. Liu[b], R. Conley[b], A. T. Macrander[b], J. Maser[b], S. Bajt[c], and H. N. Chapman[c]

[a]Materials Science Division, Argonne National Laboratory, Argonne, IL 60439

[b]Advanced Photon Source, Argonne National Laboratory, Argonne, IL 60439

[c]Lawrence Livermore National Laboratory, Livermore, CA 94550

ABSTRACT

Zone plates with depth to zone-width ratios as large as 100 are needed for focusing of hard x-rays. Such high aspect ratios are challenging to produce by lithography. We are investigating the fabrication of high-aspect-ratio linear zone plates by multilayer deposition followed by sectioning. As an initial step in this work, we present a synchrotron x-ray study of constant-period multilayers diffracting in Laue (transmission) geometry. Data are presented from two samples: a 200 period W/Si multilayer with *d*-spacing of 29 nm, and a 2020 period Mo/Si multilayer with *d*-spacing of 7 nm. By cutting and polishing we have successfully produced thin cross sections with section depths ranging from 2 to 12 μm. Transverse scattering profiles (rocking curves) across the Bragg reflection exhibit well-defined interference fringes originating from the depth of the sample, in agreement with dynamical diffraction theory for a multilayer in Laue geometry.

Keywords: x-ray optics, multilayer, Laue diffraction, focusing

1. INTRODUCTION

The Rayleigh criterion gives the best possible spatial resolution of an optic as 0.61λ/NA, where λ is the wavelength and NA is the numerical aperture.[1] According to this principle hard x-rays can be focused to very small spot sizes, on the order of their wavelength (< 1 nm), if optics with reasonably large NA and low aberrations can be produced. Although the question has been raised as to whether optics capable of focusing x-rays to spots smaller than 10 nm are theoretically possible using real materials[2], the inability to manufacture efficient optical structures for hard x-rays having NA larger than about 0.001 has placed an even more severe practical limitation on focus spot sizes obtained. Focus spot sizes of 50-100 nm have recently been reported for λ ~ 0.1 nm using Fresnel zone plates[3] and Kirkpatrick-Baez mirrors.[4] In these cases aberrations were sufficiently small that performance near the Rayleigh limit was obtained. To achieve significantly better resolution, higher NA optics will be required, such as Fresnel zone plates with smaller outermost zone widths. High efficiency for hard x-rays requires that the depth of the zone plate along the beam direction remain relatively large (e.g. several microns for Au at λ = 0.1 nm). Thus decreasing the focal spot size requires increasing the aspect ratio (depth to zone-width ratio) of the structure.[5] The inability of lithographic techniques to produce very small zones with sufficiently large aspect ratio is the current technological limit to hard x-ray zone plate performance. Although continuing advancement in e-beam and pattern transfer techniques is enabling progress, it may be exceedingly difficult to fabricate efficient hard x-ray zone plates with a spatial resolution smaller than 30 nm using lithography.[6]

The motivation for this work is the potential for an alternative zone plate fabrication technique, sectioning of a multilayer film, to provide structures with much higher aspect ratios and thus improved resolution for hard x-ray optics. Such "sputter / slice" zone plate fabrication has been developed by several groups over the past decade[7-9], and has been particularly competitive for focusing of very high energies. Circular zone plate structures have been fabricated by depositing a multilayer with depth-graded period on the outside of a cylindrical wire, and then sectioning. Proceeding

[*] stephenson@anl.gov; phone 1 630 252-2134; fax 1 630 252-7777

significantly beyond the resolution obtained to date (e.g. ~320 nm at λ = 0.05 nm[9]) using the circular wire technique may be difficult due to increasing roughness of the layers as deposition proceeds. Our approach is to produce a linear zone plate by deposition and sectioning of a graded-period multilayer on a flat substrate.[10] The thin, outermost zones are deposited first, to minimize roughness and maximize interface position accuracy in the most sensitive region. Two sections assembled face-to-face make a complete linear zone plate, and a second assembly at right angles provides focusing to a spot. The two halves of each linear zone plate can be tilted with respect to the optical axis to optimize diffraction efficiency. Since multilayer films with low-roughness layers less than 1 nm thick are readily achievable[11], this approach has the potential for producing zone plate structures with high NA and high efficiency for hard x-ray focusing optics with unprecedented resolution. A challenging requirement of this approach is to deposit and section multilayer films that are relatively thick (several microns) with many hundreds of accurately positioned layers. In addition, the optical properties of multilayers in the Laue (transmission) geometry, also known as volume gratings, have been calculated and measured only in the soft x-ray region[12,13], but are relatively unexplored in the hard x-ray region. As an initial step, we have explored the x-ray diffraction properties of constant-period multilayers (which do not focus).

In this paper we report the transverse diffraction patterns (rocking curves) as a function of section depth of sectioned multilayers studied in Laue geometry. We find good agreement between measurements and dynamical diffraction theory, providing a solid foundation for both the design and fabrication of significantly improved hard x-ray optics.

2. EXPERIMENTAL DETAILS

Two constant-period multilayers were grown on Si(001) substrates by DC magnetron sputter deposition techniques. Multilayer A was a 200-period W/Si multilayer with a d-spacing of 29 nm, for a total thickness of 6 μm, and multilayer B was a 2020-period Mo/Si multilayer with d-spacing of 7 nm, for a total thickness of 14 μm. These may be the thickest x-ray-optical-quality multilayer films produced to date.

Multilayer A was grown at the Advanced Photon Source (APS) at Argonne National Laboratory (ANL) using a system designed for multilayer growth. The substrate moved alternately between positions above the W and Si guns. The guns were programmed to turn on 10 seconds before the substrate was moved in and turn off when the specified time is up for each layer. Growth conditions were room temperature (RT), under 2.3 mTorr of Ar gas, using a deposition rate of ~0.4 nm/s for W and ~0.6 nm/s for Si. Multilayer B was deposited at Lawrence Livermore National Laboratory (LLNL). The sputtering guns mounted on the bottom of the deposition chamber are facing up, while the substrates mounted on the rotating platter are facing down. The platter with affixed substrate spinners rotates over the sputtering targets during the deposition and the platter rotational velocity controls the individual layer thickness. The deposition run was done at ~1 mTorr of Ar gas with the applied powers of 360 W for Si and 170 W for Mo. The substrate temperature was RT.

Thin cross-sections were produced by gluing a substrate to the face of the deposited multilayer, cutting ~1 mm slices using a diamond dicing saw, and then polishing the two cut faces to the desired section depth and surface finish. Since we were interested in studying the diffraction behavior as a function of section depth, we produced intentionally "wedged" cross sections with depths varying by ~10 μm across a 2 mm length so that a single sample could be used to study a range of depths. Synchrotron x-ray scattering measurements were performed at beamline 12BM of the APS. The x-rays were focused and collimated to produce a 50 × 50 μm square incident beam. Using a Si(111) monochromator, an x-ray energy of 9.5 keV (λ = 0.131 nm) was selected. Figure 1 shows a portion of a scanning electron microscopy (SEM) image

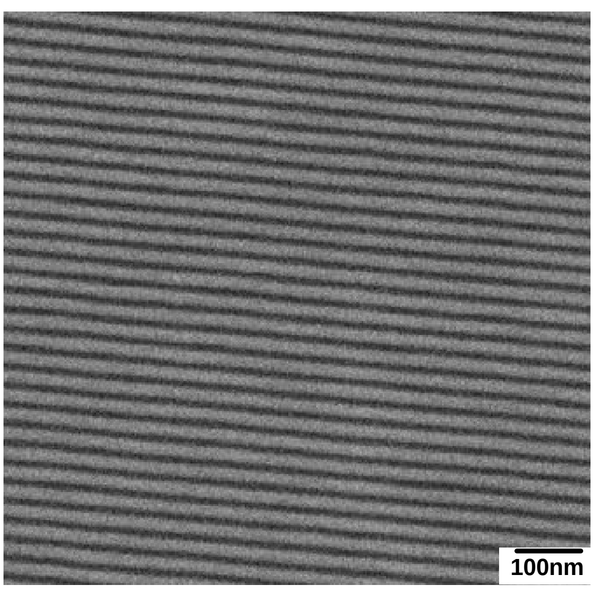

Figure 1. Cross-sectional scanning electron microscopy of multilayer A.

of a cross section of multilayer A. The layers in multilayer B were too thin to be resolved in the SEM.

The Laue diffraction geometry used is shown in Fig. 2 (inset). Here we define *z* as the layer stacking direction, *x* perpendicular to a sectioned surface, and *y* along the wedge. The x-ray scattering was mapped by scanning the scattering vector in the Q_x and Q_z directions. The dependence on section depth was determined by translating the wedge-shaped sample along the *y* direction.

3. RESULTS AND DISCUSSION

Figure 2 shows a typical radial (reflectivity) scan along Q_z at $Q_x = 0$. Absolute reflectivity was calculated from the measured intensity corrected for the fraction of the incident beam subtended by the sample. A sequence of Bragg reflections from the multilayer period is observed. The pattern is symmetric about zero, which illustrates a feature of the unusual Laue geometry: diffraction from the "top" or "bottom" of the multilayer is equivalent. Unlike the reflection geometry, there is no critical angle below which total reflection occurs. Figure 3 shows typical transverse (rocking) profiles along Q_x at the first-order Bragg reflection in Q_z, for various values of section depth. The profiles exhibit interference fringes around the central peak. The section depth *w* of the illuminated region can be obtained from the period DQ_x of the interference fringes using $w = 2p/DQ_x$. The large number of fringes indicates that the sectioning process produced smooth truncation of the multilayer with a well-defined depth. The central part of the profile displays a complex dependence on section width. The profiles for small *w* have the shape of classical Fraunhofer single-slit diffraction patterns.[1] For multilayer B, as *w* increases the intensity of the central maximum decreases relative to those of the fringe maxima. For multilayer A, the intensity at $Q_x = 0$ becomes a local minimum for values of *w* near 8 µm, and then becomes a local maximum again at larger depths. The maximum reflectivities of multilayers A and B were approximately 35% and 70% at depths of 4 and 7.5 microns, respectively.

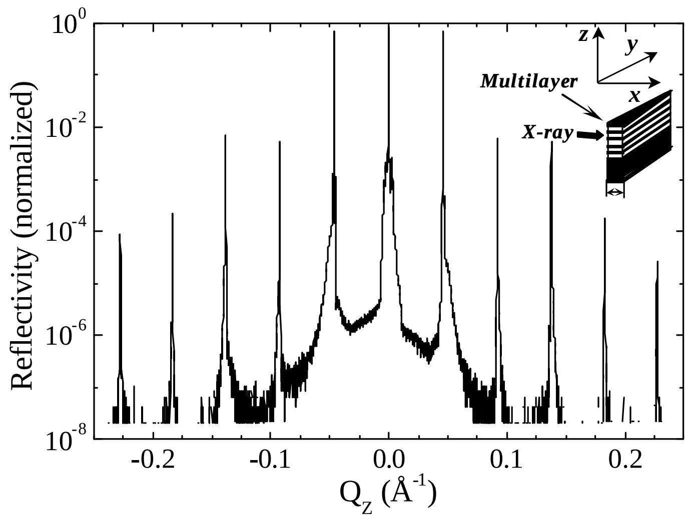

Figure 2. Typical radial scan for multilayer B, showing multiple positive and negative orders of Bragg peaks (*w* = 7.5 µm).
Inset: Schematic of Laue geometry used in this study.

A quantitative model can be developed by extending the 2-beam dynamical diffraction theory for crystals to the case of sectioned multilayers by considering the reflectivity of a centrosymmetric crystal in the symmetric Laue geometry, in the limit of small diffraction angle, which is given by[14,15]

$$R = \exp\left[\frac{2pw\,\mathrm{Im}(y_0)}{l}\right]\frac{\left|\sin\left(\frac{pwy_H}{l}\sqrt{1+h^2}\right)\right|^2}{\left|1+h^2\right|}, \qquad (1)$$

where *h* is related to the transverse wavenumber Q_x by $h = Q_x\, l / 2\, p\, y_H$, and the normalized structure factors in the forward and diffracted-beam directions, y_0 and y_H, are given by

$$y_H = \frac{2\Delta n \sin(pLx)}{pL},$$

$$y_0 = 2(\langle n\rangle - 1)\,.$$

Here *n* is the refractive index, $\langle\ \rangle$ represents the mean of the two layers in the multilayer, e.g. $\langle n\rangle = xn_1 + (1-x)n_2$, *D* represents the difference between the two layers, e.g. $Dn = n_1 - n_2$, *x* is the volume fraction of layer 1, and *L* is the order

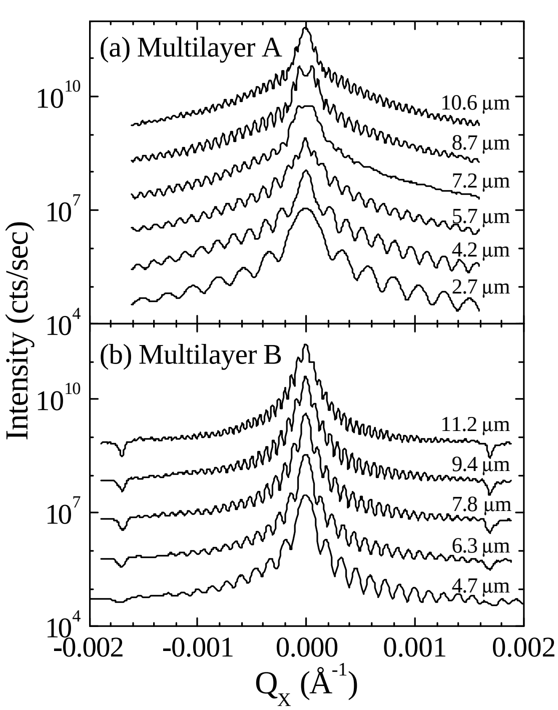

Figure 3. Measured transverse profiles (rocking curves) through the *001* reflection for various section depths. Profiles are offset by factors of 10 for clarity.

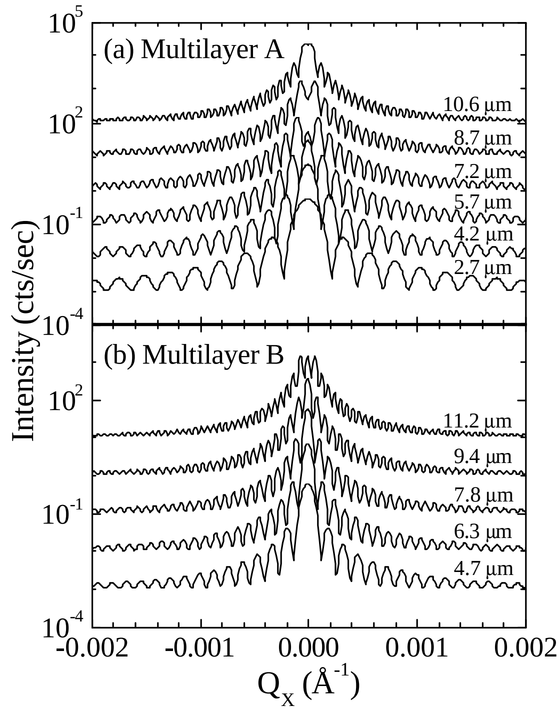

Figure 4. Calculated transverse profiles corresponding to Fig. 3, using two-beam theory. For multilayer A, x=0.6; for multilayer B, x=0.5.

of the *00L* Bragg peak. The refractive indices of each the layers are complex numbers given by $n = 1 - d - ib$, where d and b depend on material and photon energy.[16] Rocking curves calculated using Eq. (1) (assuming layer densities equal to standard values for pure elements) are shown in Fig. 4. Note that these curves are independent of multilayer period. At the center of the rocking curve, where h = 0, the reflectivity as a function of section depth w can be expressed as

$$R = \exp\left[-\frac{4pw\langle b\rangle}{l}\right]\left(\sin^2\left[\frac{2w\sin(pLx)\Delta d}{lL}\right] + \sinh^2\left[\frac{2w\sin(pLx)\Delta b}{lL}\right]\right). \qquad (2)$$

The $\sin^2$ term gives the oscillatory *pendellosung* component, with a period $Dw = p\,lL|2Dd\,\sin(pLx)|^{-1}$, while the $\sinh^2$ term gives the anomalous transmission (Borrmann effect) for samples with large section depth.[15] Note that the *pendellosung* period depends on Dd, and is thus a direct measure of the scattering contrast of the multilayer.

Because the small section depth broadens the rocking curves, and the diffraction angles are small, the rocking curves show effects of multiple scattering. This can be seen clearly in Fig. 3(b), where there are symmetrically-placed dips at $Q_X = \pm 0.0017$ Å^{-1} in the tails of the *001* rocking curves. These features arise at the points where the crystal has been rotated by $Dq = \pm 2q_B$ from the center of the reflection, where q_B is the Bragg angle for the reflection. In the symmetric Laue geometry, the angle between the incident and exit beam is $2q_B$. Therefore, as shown in Table 1, either the incident

Table 1. Explanation for multiple scattering at $Dq = \pm 2q_B$.

	Angle with respect to Bragg planes:	
Rocking angle Dq	Incident beam	Exit beam
$-2q_B$	$-q_B$	$-3q_B$
0	q_B	$-q_B$
$2q_B$	$3q_B$	q_B

or the exit beam makes the angle θ_B with respect to the Bragg planes at these points, so that strong multiple scattering off the same set of Bragg planes occurs. The value of Q_X corresponding to $\Delta\theta = \pm 2\theta_B$ for the *(001)* planes is given by $Q_X = \pm 2\pi\lambda/d^2$, where d is the multilayer period. For multilayer B at 9.5 keV, this gives $Q_X = \pm 0.00167$ Å^{-1}, as observed. For multilayer A at 9.5 keV, this gives $Q_X = \pm 0.00010$ Å^{-1}. These positions are so close to the central peak that the multiple scattering features cannot be resolved. Instead, they contribute to the unusual shapes of the central peak.

In general, one must also consider multiple scattering corresponding to the excitation of other Bragg peaks, i.e. harmonics of the *001* fundamental. Since the angles are small, the Bragg angles of the harmonics are integer multiples of the fundamental Bragg angle. Thus one expects strong multiple scattering at rocking angles that are multiples of the (001) θ_B. When the sample depth is small, so that the width of the central peak, $|\Delta\theta| = d/w$ is equal to or larger than the fundamental Bragg angle $\theta_B = \lambda/2d$, this multiple scattering is important even at the center of the rocking curve. The condition for this to occur can be written as $d^2 > \lambda w/2$. This occurs for multilayer A, but not for multilayer B, in this study.

4. CONCLUDING REMARKS

In summary, we have successfully fabricated high-quality, constant-period volume gratings with a high aspect ratio suitable for efficient diffraction of hard x-rays using deposition and sectioning of multilayer films. The measured x-ray scattering shows thickness fringes in the rocking curves, in agreement with 2-beam dynamical diffraction theory for the Laue geometry. In the future we plan to model the multiple scattering effects observed for sample A using the n-beam, coupled-wave theory treatment.[17] The results of this study will allow the design and fabrication of hard-x-ray focusing optics using deposition and sectioning of graded-period multilayers.

ACKNOWLEDGMENTS

The authors would like to thank Dr. M. Zurbuchen for SEM measurements, and the BESSRC beamline staff for capable assistance. Work performed under the auspices of the U.S. Department of Energy by ANL under contract W-31-109-ENG-38 and by LLNL under contract W-7405-ENG-48. One of the authors (H.C.K.) also acknowledges support from Korea Science and Engineering Foundation (KOSEF) by the Post-doctoral Fellowship Program.

REFERENCES

1. M. Born and E. Wolf, *Principles of Optics*, 6th ed., (Pergamon, New York, 1980).
2. C. Bergemann, H. Keymeulen, and J. F. van der Veen, Phys. Rev. Lett. 91, 204801, (2003).
3. S. Wang, F. Duewer, S. Kamath, C. Kelly, A. Lyon, K. Nill, D. Scott, D. Trapp, Y. Wenbing, S. Neogi, M. Kuhn, C. Bennet, P. Coon, and Y. Souping, Proc. of the 28th Int. Symp. for testing and failure analysis, 227 (2002).
4. K. Yamamura, K. Yamauchi, H. Mimura, Y. Sano, A. Saito, K. Endo, A. Souvorov, M. Yabashi, K. Tamasaku, T. Ishikawa, and Y. Mori, Rev. Sci, Instrum. 74, 4549 (2003).
5. C. David, B. Nohammer, E. Ziegler, Appl. Phys. Lett. 79, 1088 (2001); B. Nohammer, J. Hoszowska, H.-P. Herzig, and C. David, J. Phys. IV 104, 193 (2003).
6. M. Peuker, Appl. Phys. Lett. 78, 2208 (2001).
7. R.M. Bionta, K.M. Skulina, and J. Weinberg, Appl. Phys. Lett. 64, 945 (1994).
8. B. Kaulich, *Ph.D thesis*, University of Goettingen, Germany (1996).
9. N Kamijo *et al*., Rev. Sci. Instrum. 74, 5101 (2003); S. Tamura *et al*., J. Synchrotron Radiation 9, 154 (2002).
10. S. Vogt, J. Maser, and G.B. Stephenson, to be published in Proc. 8th Int. Conf. on Synchrotron Radiation Instrumentation, (2003).
11. C. Liu, R. Conley, A.T. Macrander, T. Graber, Ch. Morawe, C. Borel, and E. Dufresne, "Small d-spacing WSi_2/Si multilayers", to appear in SPIE Conf. Proc.Vol. 5537., SPIE 49th Annual Meeting, (2004).
12. V. E. Levashov and A. V. Vinogradov, Appl. Optics 32, 1130 (1993).
13. D. Hambach, G. Schneider, and E.M. Gullikson, Opt. Lett. 26, 1200 (2001).

14. W. H. Zachariasen, *Theory of X-ray Diffraction in Crystals*, (Constable and Co., London, 1945), p. 113.
15. B. W. Batterman and H. Cole, Rev. of Mod. Phys. 36, 681 (1964).
16. B. L. Henke, E. M. Gullickson, and J. C. Davis, At. Data Nucl. Data Tables 54, 181 (1993).
17. J. Maser and G. Schmahl, Opt. Commun. 89, 355 (1992).